

# A Proposed Compact Broadband Meander Antenna for RFID Applications

Amin Al Ka'bi

Australian University, Kuwait  
Email: a.kabi@au.edu.kw

**Abstract**—Radio Frequency Identification technology aims at identifying and tracking objects labeled with tags. To achieve this goal, the need for antennas with certain characteristics and specifications becomes of great importance. In this research work, a proposed compact broadband meander antenna for Radio Frequency Identification Applications is presented. In the proposed model of the antenna, the inductive strips are bent to generate capacitive effects between them. To achieve an acceptable impedance matching at a frequency of 876MHz between the antenna and the receiving microchip of model “NXP UCODE G2XL”, shorting lines created along the antenna structure together with a T-shaped matching circuit are used. This proposed design of the antenna results in a compact size antenna ( $75 \times 25 \times 1.6 \text{ mm}^3$ ) with a resonance frequency that lies in the European band of 867MHz, and it has an input impedance of  $Z = 16 - j156 \Omega$ . The antenna is made from copper strip with a thickness of  $35 \mu\text{m}$  and fabricated on an FR4 epoxy substrate with a thickness of 1.6 mm. This paper presents the proposed antenna simulation results performed in various situations and conditions. The antenna performance is investigated in terms of various aspects such as gain, radiation pattern, return loss, and input impedance.

**Keywords**—Meander antenna, radio frequency identification, dipole meander, wireless, radiation pattern, return loss

## I. INTRODUCTION

Radio Frequency Identification (RFID) technology is currently being used in identifying and tracking tagged objects or human beings by transmitting electromagnetic waves at Radio Frequency (RF). This emerging technology shows high degree of compatibility with many existing industries and relevant industries in this field. The RFID system consists mainly of two basic components, the reader, and the tag, besides a data processor for reading and processing data related to the targeted object [1]. To enable capturing and storing data related to the targeted object, an antenna is mounted to microchip of model “NXP UCODE G2XL”. In this system, the RFID reader transmits an exploration signal, and the antenna receives the scattered signal back from the tagged object that contains the data saved into the microchip it connected to. The basic principle of operation of passive RFID UHF is illustrated in Fig. 1. The main three

categories of RFID tags are active, passive, and semi-passive tags [2]. They can be recognized based on their energy supplies and their communication algorithms when the tag is positioned in the detection range of the RFID reader. Moreover, according to International Industrial, Scientific, and Medical (ISM) standards RFID UHF can be subclassified into various bands according to their region of the world. Diverse UHF bands can be allocated based on the effective regulations and policies in the region of operation. For covering the whole passive UHF band, the range of frequencies should lie in the range 860 MHz to 960 MHz [3]. Due to their high data reading rates, and high communication speeds, RFID UHF systems are widely used in detection and tracking technology [4, 5].

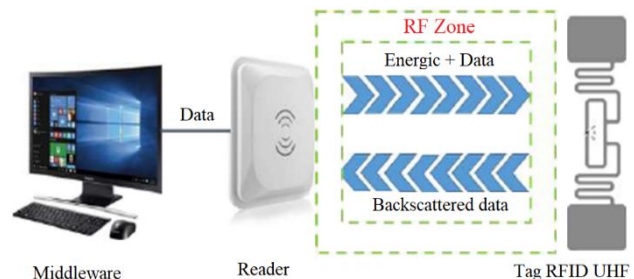


Figure 1. Principle of operation of passive RFID UHF system.

Literature review introduced different techniques for designing antennas of RFID tags with different types and sizes. For example, Paredes and Zamora *et al.* [2] presented a plane dipole antenna with pair of two elements loaded at its ends., while Ramirez and Rojas-Nastrucci *et al.* [4] and Khan and Al-Hadi *et al.* [6] presented two designs of small-scale copper RFID dipole antennas, the first one is fabricated on FR4 epoxy with spiral inductors at its ends and the second one is fabricated on PET and it has a volume of  $822.2 \times 35.1 \times 0.059 \text{ mm}^3$  with relatively higher gain. On the other hand, a meander single-band dipole antenna operating in free space is proposed by Ka'bi [7], while Liu, Yang, and Ku [1] proposes a meander dual-band RFID antenna operating in various media.

In this paper, a proposed design of RFID compact size antenna with a volume of  $75 \times 25 \times 1.6 \text{ mm}^3$  is presented. It is a meandering dipole antenna made from copper and fabricated on FR4 epoxy, with two stub pairs are mounted on the two sides of the matching circuit to enable the antenna to resonate at the desired operating frequency. The remaining parts of this paper are arranged as follows:

Manuscript received August 15, 2022; revised September 16, 2022; accepted January 1, 2023.

Section II explains the parameters of the antenna design, Section III illustrates the performance of the antenna (mainly its resonant frequency, and input impedance) versus the variations in the design parameters, Section IV illustrates the performance of the proposed antenna in free space and in other types of environments. The main conclusions of this paper are included in the conclusions section.

## II. PARAMETERS OF PROPOSED ANTENNA

Fig. 2 depicts the proposed antenna design. It is mainly a meandering dipole with a height of 1.6 mm and made from copper with stub pairs mounted on its ends, and it fabricated on an FR4 epoxy substrate with  $\epsilon_r = 4.4$ ; and  $\tan \sigma = 0.02$ . There is a good impedance matching between the proposed antenna and the receiving microchip of the model “IC NXP UCODE G2XL” with a TSSOP8 package. The power threshold sensitivity of this microchip is -17 dBm and an input impedance of  $Z_c = 16 - j 156 \Omega$  [8]. To provide impedance matching between the microchip and the proposed antenna, a T-shaped matching network is connected to the inductive strips on both sides of the antenna.

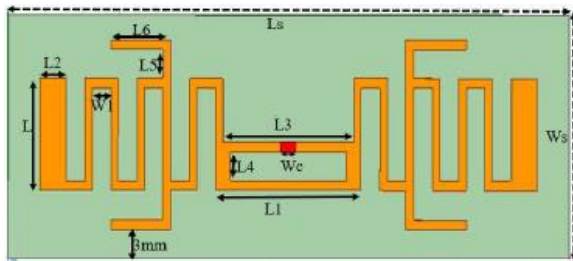


Figure 2. Proposed antenna design.

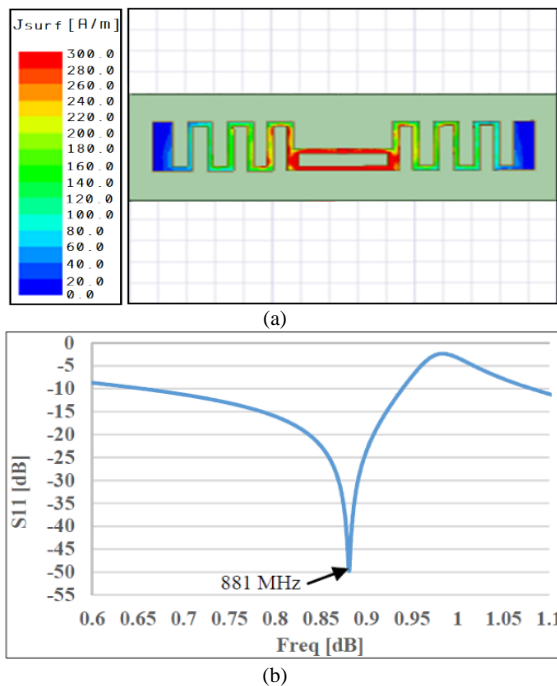


Figure 3. Simulation of antenna prototype 1 (a) Distribution of current density (b) Reflection coefficient.

The proposed antenna design is performed in three stages:

- Firstly, a basic dipole antenna with meandering shape is designed to resonate at a frequency of 881.1 MHz with an  $S_{11}$  parameter of -49.7674 dB where Fig. 3a. depicts surface current density and its distribution throughout the whole radiating sections. Fig. 3b illustrates the  $S_{11}$  parameter versus frequency.
- Secondly, to concentrate the current density in the central area of the radiating section, a short circuit is implemented on both sides of the antenna. This configuration causes the proposed antenna to resonate at 861.1 MHz with  $S_{11}$  parameter of -33.0473 dB as illustrated in Fig. 4a.
- Thirdly, another two stubs are lowered to form two pairs of short circuits to compensate for the losses. This step allows the antenna to resonate at 867 MHz, and to provide matching with the conjugate of the microchip impedance with  $S_{11}$  parameter of -44.1573 dB as illustrated in Figs. 5 (a, b).

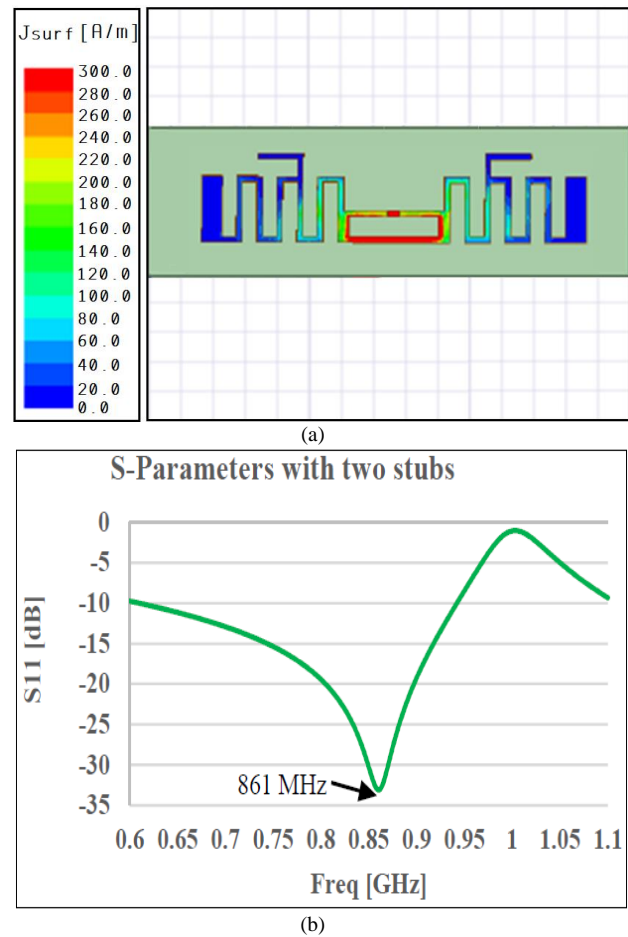


Figure 4. Simulation of antenna prototype 2 (a) Distribution of current density (b) Reflection coefficient.

It is worth mentioning that in all these cases, it is observed that the antenna gain remained constant.

III. ANALYSIS OF DESIGN PARAMETRS

The analysis of the effect of design parameters on the performance of the antenna enables determining the values resonance frequencies and matching impedances.

Fig. 5a illustrates the effect of varying the lengths of the induction lines L between 11 mm and 12 mm. Figs. 5 (a-c) show an increase in the inductive effect on the reflection coefficient and the input impedance of the antenna, besides a significant decrease in the resonant frequency is observed, while the best impedance match occurs when L=11.5 mm.

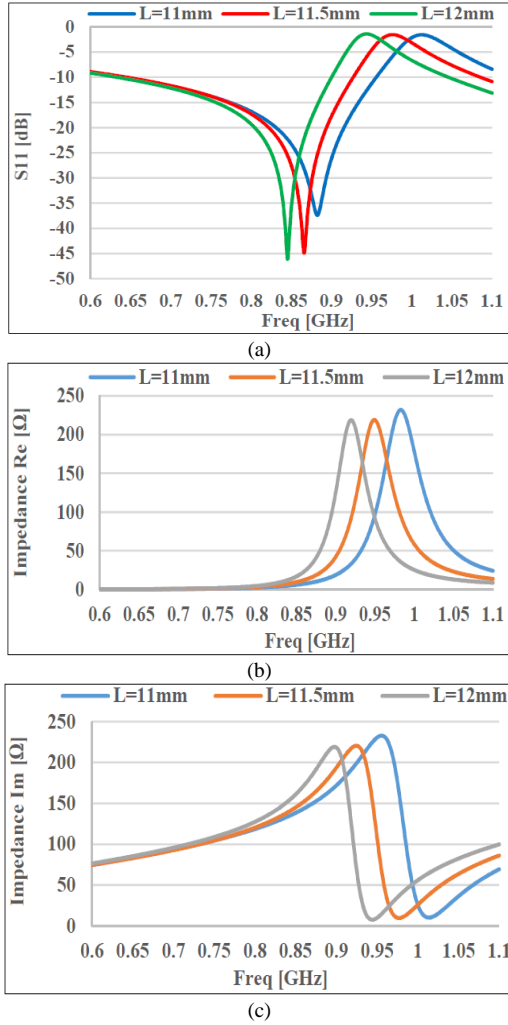


Figure 5. Antenna parameters versus frequency for different values of L (a) Reflection coefficient (b) Antenna resistance, (c) Antenna reactance.

The changes in the antenna parameters cause change in antenna input impedance at certain frequency, and hence, to match the antenna at the same impedance the operating frequency should be adjusted which results in a new resonance frequency. Fig. 6 depicts the effect of varying the width L2 of the longest line between 3mm and 4.5mm. This variation results in better antenna adaptation which allows varying its resonance frequency, due to its inductive effect on the antenna, which in turn enables locating the best matching impedance. The resonance

frequency of 867 MHz is achieved when L2=3.5 mm as depicted in Fig. 6a.

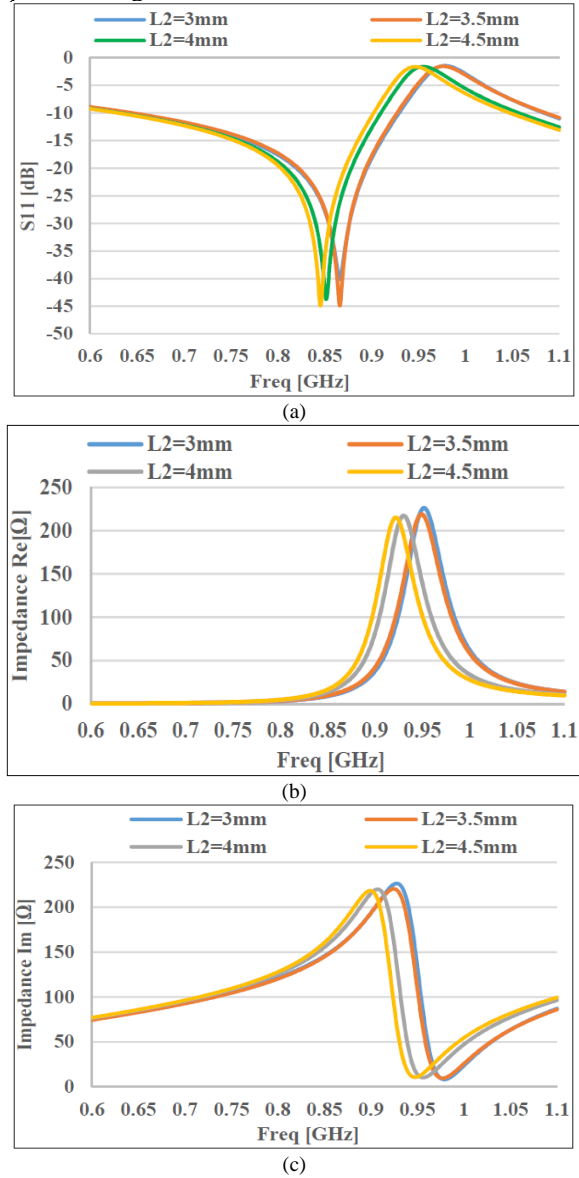


Figure 6. Antenna parameters versus frequency for different values of L2 (a) Reflection coefficient (b) Antenna resistance, (c) Antenna reactance.

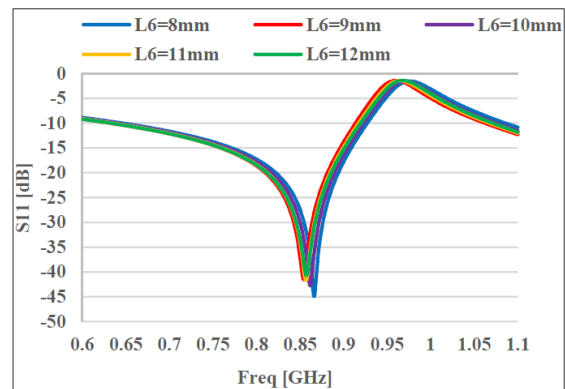


Figure 7. Reflection coefficient vs. frequency for different values of L6.

Fig. 7 depicts the effect of varying the length L6. It is observed that this variation does not have significant effect on the antenna performance.

As a result of the parametric analysis of the proposed model of the antenna, all the optimal values of the corresponding antenna parameters are determined, and hence best antenna performance is achieved. A summary of the proposed antenna parameters is included in Table I.

TABLE I. PROPOSED ANTENNA PARAMETERS

Parameters	$L_s$	$W_s$	$L$	$L1$	$L2$
Values (mm)	75	25	11.5	19.5	3.5
Parameters	$L3$	$L4$	$L5$	$L6$	$W1$
Values (mm)	17.5	3	3	8	2.5

IV. SIMULATION RESULTS OF THE PROPOSED ANTENNA MODEL

A. Simulation Results in Free Space

In this section, the simulation results of the proposed antenna model are presented in terms of return loss, input impedance, and radiation pattern. Fig. 8a illustrates the variation of reflection coefficient of the proposed antenna model versus the operating frequency, while Fig. 8b shows its input impedance versus frequency. It is found that the proposed antenna resonates at 867 MHz with a return loss of  $S_{11} = -44.1573$  dB due to the matching input impedance of  $Z_a = 14.7376 + j157.4704 \Omega$  which is very close to the conjugate of the microchip impedance of  $Z_c^* = 16 + j156 \Omega$ .

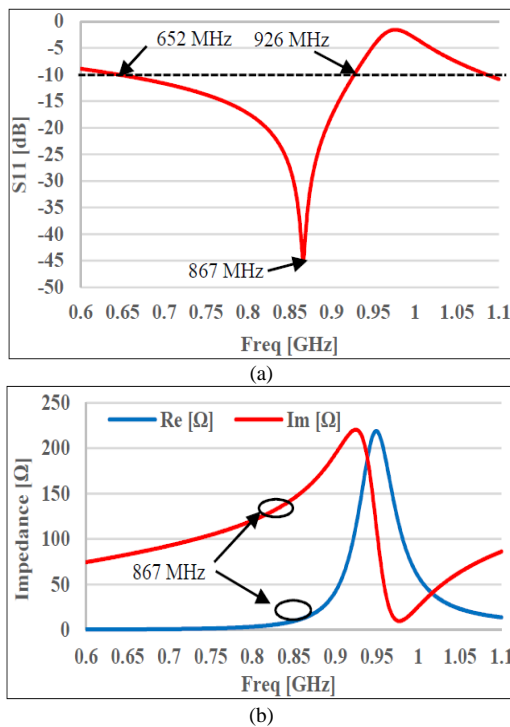


Figure 8. Performance of proposed antenna model (a) Reflection coefficient (b) input impedance.

The transmission coefficient of the antenna is defined as the amount of power delivered to the microchip to the power received by the antenna. If the return loss is known, the transmission coefficient can be calculated from Eq. 1 as follows [9]:

$$\tau = 1 + |\Gamma|^2 = \frac{4R_c R_a}{|Z_c + Z_a|^2} \quad 0 \leq \tau \leq 1 \quad (1)$$

where  $\tau$  is the reflection coefficient,  $Z_a = R_a + jX_a$ ,  $Z_c = R_c + jX_c$  are the impedances of the antenna and the microchip respectively.

Using Eq. (1) the transmission coefficient  $\tau$ , it is found that  $\tau = 99.058\%$ . which shows an excellent impedance matching between the proposed antenna model and the microchip, and hence almost all the power received by the antenna is delivered to the microchip with no significant losses.

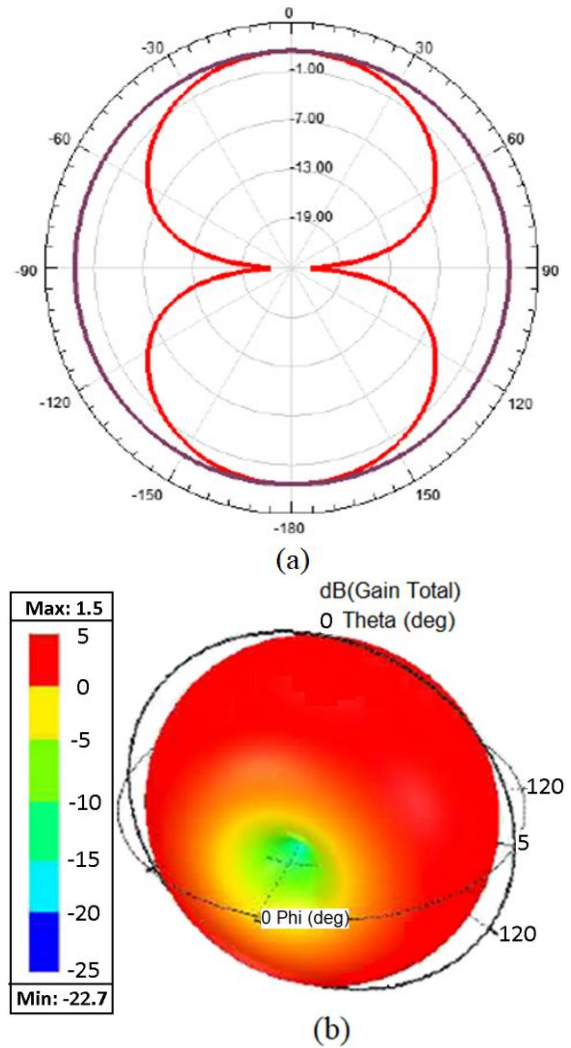


Figure 9. (a) Radiation pattern and (b) Gain of proposed antenna.

On the other hand, Fig. 9 illustrates the antenna gain two and three dimensions. The importance of antenna gain emerges from its direct impact on the detection range of the tag. It is found a gain of 1.5 dB is achieved at a

frequency of 876 MHz. The antenna efficiency can be determined from Eq. (2).

$$\eta = \frac{G}{D} \quad (2)$$

where  $G$  is the antenna gain, and  $D$  is its directivity. Hence an efficiency of 91.2% is achieved at a directivity of 1.9 dB for the dipole tag antenna.

**B. Performance of Proposed Antenna Using Different Surfaces**

The effect of the type of the antenna surface on its performance is investigated in this section. For this purpose, different types of surfaces are used, such as polyethylene terephthalate PET with  $\epsilon_r = 3$  and  $\tan \sigma = 0.002$  [10], wood with  $\epsilon_r = 1.7$  and  $\tan \sigma = 0.036$  [11], and foam with  $\epsilon_r = 1.03$  and  $\tan \sigma = 0.0001$  [12]. Table II shows the thicknesses of these surfaces.

Fig. 10 shows the antenna reflection coefficients using these surfaces versus the operating frequency. From the graph, it can be concluded that wood and glass surfaces have significant effect on the resonance frequency of the antenna due to their high relative permittivity, while foam and polyester have less effect due to their low relative permittivity which is very close to free space.

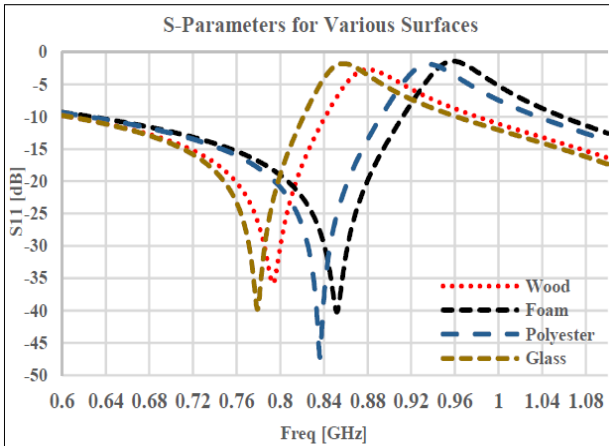


Figure 10. Effect of antenna surface on its resonance frequency.

Table II shows the antenna gains and reading range when different types of surfaces are used. The results show that the best gains and longest reading ranges were obtained by using wood, glass or plastic surfaces compared to free space. The reading range is the maximum distance at which the reader can detect the tag on the target, and it can be calculated from Eq. (3) as follows [13-16]:

$$r_{max} = \frac{\lambda}{4\pi} \sqrt{\frac{P_{EIRP} G_R}{P_{th}}} \quad (3)$$

where  $P_{EIRP} = P_t \cdot G_t$  is the reader effective isotropic radiated power,  $P_t$  is the transmitted power,  $G_t$  is the gain, and  $P_{th}$  is the minimum power threshold required to activate the FFID tag microchip.

TABLE II. ANTENNA PERFORMANCES FOR VARIOUS SURFACES

Surfaces	Gain (dB)	Read Range (m)	Thickness (mm)
Foam	1.5	12.6	5
Glass	2.1	13.5	1.5
Polyester	1.7	12.8	0.5
Wood	0.65	11.4	10

The results show that the reading range of the proposed antenna is at least 10 m regardless of the surface used, since the type of the used surface does not affect the radiation pattern of the antenna. As a conclusion, the proposed antenna model functions well in various types of environments.

To investigate the performance of the proposed tag antenna in diffusive environments, bottle filled with liquid is used as a surface for the antenna as depicted in Fig. 11. The bottle is filled with different types of liquids such as water ( $\epsilon_r = 81$ ;  $\tan \sigma = 0$ ), vinegar ( $\epsilon_r = 76$ ;  $\tan \sigma = 13.7$ ), orange juice ( $\epsilon_r = 78$ ;  $\tan \sigma = 12.5$ ), and oil ( $\epsilon_r = 3.2$ ;  $\tan \sigma = 0.1$ ). The antenna is mounted vertically on the PET bottle with dimensions of  $250 \times 80 \times 60 \text{ cm}^3$  filled with the liquid.

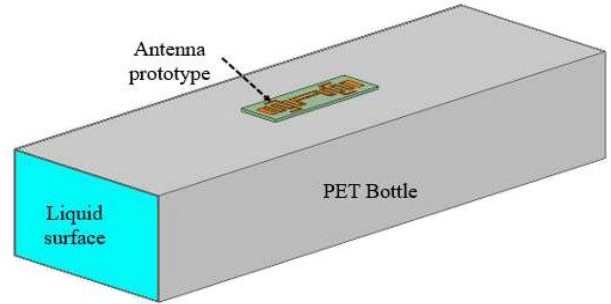
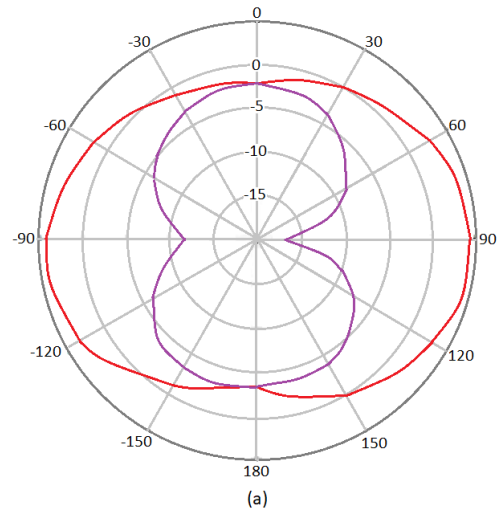


Figure 11. Proposed antenna placed on a plastic bottle containing liquid.

Fig. 12 illustrates the radiation patterns of the proposed antenna with azimuth angles of  $\Phi = 0^\circ$  and  $\Phi = 90^\circ$  and variable elevation angle  $\theta$  between  $0^\circ$  and  $180^\circ$ .



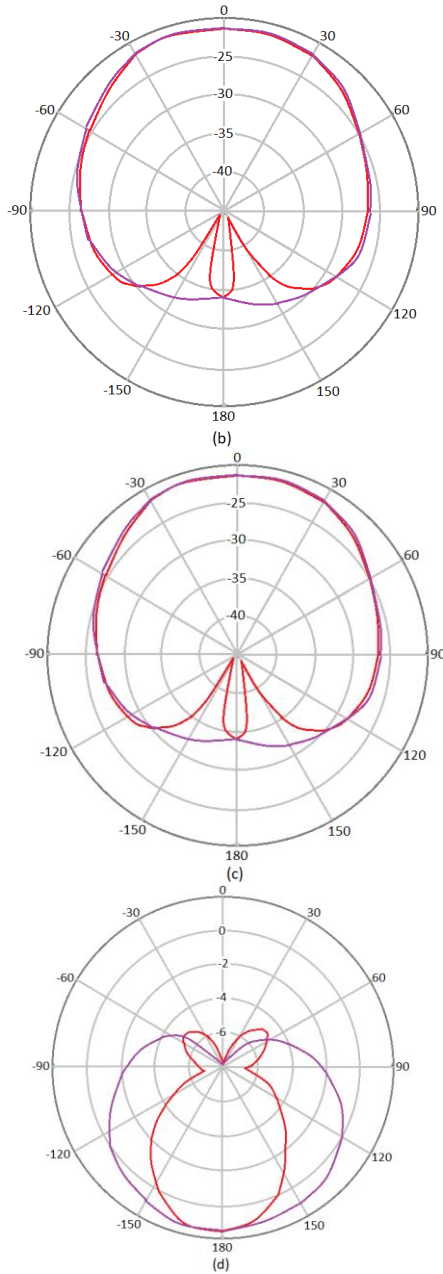


Figure 12. Radiation pattern and gain of the proposed antenna using various liquid surfaces (a) water, (b) orange juice, (c) vinegar, and (d) oil.

It is observed that different radiation patterns are obtained depending on the type of the liquid in the bottle. For example, with the bottle filled with water, the maximum obtained antenna gain 4.5 dB at  $\theta = 90^\circ$  in the  $x$ - $y$  plane, while it is -2.5 dB at  $\theta = 0^\circ$ , as depicted in Fig. 12a. In the case of vinegar and orange juice liquids, it is observed that the radiation pattern converts to directional along the  $+z$  axis (i.e., at  $\theta = 0^\circ$ ) with very low gain as illustrated in Fig. 12b and Fig. 12c.

The bottle filled with oil has significant effect on the radiation pattern in terms of converting it to directional along the negative  $z$  axis with low gain, which in turn decreases its reading range. Table III. shows the

comparison of the proposed antenna with the existing antenna designs in the literature. It can be seen that the proposed antenna provides the highest gain compared to other proposed designs presented in the literature.

TABLE III. COMPARISON OF THE PROPOSED ANTENNA WITH OTHER STUDIES IN THE LITERATURE

Reference	Antenna Size (mm <sup>2</sup> )	Gain (dBi)
(Jha, Bukhari et al. 2018) [16]	120×65	0.867
(Srivastava, Saurabh et al. 2019) [17]	100×40	0.503
(Kuo and Wong 2003) [18]	70×50	0.85
(Wu, Hsiao et al. 2004) [19]	75×75	1.3
(Naidu, Kumar et al. 2019) [20]	10×19	0.87
(Liu, xu et al. 2018) [21]	12.5×13	0.56
Proposed Antenna	75×25	1.5

## V. CONCLUSION

In this research work, a proposed compact meandering shape dipole antenna is proposed for RFID applications. The purpose of this antenna is to enable reading the tags on the targeted objects. Various simulations of the performance of the antenna are carried out in various environments. It is found that the proposed antenna provides excellent performance in free space with tag reading range of 12.6 m and with an excellent impedance matching with the receiving microchip of model NXP UCODE G2XL IC at an operating frequency of 867MHz. Moreover, it is found that the antenna provides good performance in other media such as plastic, glass, wood, and foam. On the other hand, the performance is significantly degraded when liquid surfaces are used such as bottles filled with water, vinegar, orange juice, etc. This degradation in performance results in higher impedance mismatches, low gains, and low reading ranges of the RFID tags. However, the overall performance of the antenna with liquid surfaces can be enhanced by using appropriate ground plane, and the problem of back radiation when oil medium is used can be mitigated by using multiple antenna prototypes which enables the radiation in the desired direction.

## CONFLICT OF INTEREST

The author declares no conflict of interest.

## AUTHOR CONTRIBUTIONS

This paper has one author, and he approved the final version.

## REFERENCES

- [1] H. W. Liu, C. F. Yang, and C. H. Ku, "Novel miniature monopole tag antenna for UHF RFID applications," *IEEE Antennas and Wireless Propagation Letters*, vol. 9, pp. 363-366, 2010.
- [2] F. Paredes, G. Zamora, F. J. Herraiz-Martínez, F. Martín, and J. Bonache, "Dual-band RFID tags based on folded dipole antennas

- loaded with spiral resonators,” in *Proc. 2012 IEEE International Workshop on Antenna Technology (iWAT)*, 2012, pp. 136-139.
- [3] M. R. Basheer and S. Jagannathan, “Localization of RFID tags using stochastic tunneling,” *IEEE Transactions on Mobile Computing*, vol. 12, no. 6, pp. 1225-1235, 2013.
- [4] R. A. Ramirez, E. A. Rojas-Nastrucci, and T. M. Weller, “UHF RFID tags for On-/Off-Metal applications fabricated using additive manufacturing,” *IEEE Antennas and Wireless Propagation Letters*, vol. 16, pp. 1635-1638, 2017.
- [5] K. Zannas, H. E. Matbouly, Y. Duroc, and S. Tedjini, “A flipping UHF RFID sensor-tag for metallic environment compliant with ETSI/FCC bands,” *IEEE Transactions on Antennas and Propagation*, vol. 69, no. 3, pp. 1283-1292, March 2021.
- [6] A. A. Ka’bi, “Proposed antenna design for IoT and 5G-WiFi applications,” in *Proc. 2022 IEEE World AI IoT Congress (AIoT)*, 2022, pp. 786-790.
- [7] R. Khan, A. A. Al-Hadi, P. Soh, M. Ali, O. Owais, and I. Islam, “Multiband monopole antenna with minimized ground plane influence for portable devices,” *Iet. Microwaves Antennas & Propagation*, vol. 11, pp. 1829-1835, 2017.
- [8] F. Sakai, M. Makimoto, and K. Wada, “Multimode stepped impedance resonators and their application in chipless RFID tags,” in *Proc. 2016 46th European Microwave Conference (EuMC)*, 2016, pp. 604-607.
- [9] A. Buffi, B. Tellini, A. Motroni, and P. Nepa, “A phase-based method for UHF RFID gate access control,” in *Proc. 2019 IEEE International Conference on RFID Technology and Applications (RFID-TA)*, 2019, pp. 131-135.
- [10] B. Dang, *et al.*, “In-body/out-body dual-use miniaturized RFID tag system using 920MHz/5.02GHz bands,” in *Proc. 2020 IEEE International Symposium on Radio-Frequency Integration Technology (RFIT)*, 2020, pp. 148-150.
- [11] A. A. Ka’bi, “Design of a microstrip dual band fractal antenna for mobile communications,” in *Proc. 2022 IEEE International Black Sea Conference on Communications and Networking (BlackSeaCom)*, Sofia, Bulgaria, June 2022, pp. 85-90.
- [12] A. A. Ka’bi, “A proposed antenna design for IoT and 5G-WiFi applications,” *Telecommunications and Radio Engineering*, vol. 81, no. 6, pp. 15-22, 2022.
- [13] J. Kulkarni, C. Y. D. Sim, and V. Deshpande, “Low-profile, compact, two port MIMO antenna conforming Wi-Fi-5/Wi-Fi-6/V2X/DSRC/INSAT-C for wireless industrial applications,” in *Proc. 2020 IEEE 17th India Council International Conference (INDICON)*, 2020, pp. 1-5.
- [14] A. A. Ka’bi, “Design of an electromagnetic frequency tunned antenna for mobile communications,” *Wireless Personal Communications*, vol. 118, no. 4, pp. 2601–2610, 2021.
- [15] J. S. Kulkarni and C. Y. D. Sim, “Low-Profile, multiband & wideband ‘C-Shaped’ monopole antenna for 5G and WLAN applications,” in *Proc. 2020 International Conference on Radar, Antenna, Microwave, Electronics, and Telecommunications (ICRAMET)*, 2020, pp. 366-371.
- [16] K. R. Jha, B. Bukhari, C. Singh, G. Mishra, and S. K. Sharma, “Compact planar multistranded MIMO antenna for IoT applications,” *IEEE Transactions on Antennas and Propagation*, vol. 66, no. 7, pp. 3327-3336, 2018.
- [17] B. Satyanarayana, *et al.*, “Side-Edge frame coupled-fed printed eight-port MIMO antenna array for sub-6 GHz 5G smartphone applications,” in *Proc. IEEE MTT-S International Microwave and RF Conference (IMARC)*. IEEE, 2019.
- [18] Y. L. Kuo and K. L. Wong, “Printed double-T monopole antenna for 2.4/5.2 GHz dual-band WLAN operations,” *IEEE Transactions on Antennas and Propagation*, vol. 51, no. 9, pp. 2187-2192, 2003.
- [19] J. W. Wu, *et al.*, “Dual broadband design of rectangular slot antenna for 2.4 and 5 GHz wireless communication,” *Electronics Letters*, vol. 40, no. 23, pp. 1461-1463, 2004.
- [20] P. V. Naidu, A. Kumar, and R. Rajkumar, “Design, analysis and fabrication of compact dual band uniplanar meandered ACS fed antenna for 2.5/5 GHz applications,” *Microsystem Technologies*, vol. 25, pp. 97-104, 2019.
- [21] L. Jie, J. Li, and R. Xu. “Design of very simple frequency and polarisation reconfigurable antenna with finite ground structure,” *Electronics Letters*, vol. 54, no. 4, pp. 187-188, 2018.

Copyright © 2023 by the authors. This is an open access article distributed under the Creative Commons Attribution License ([CC BY-NC-ND 4.0](https://creativecommons.org/licenses/by-nc-nd/4.0/)), which permits use, distribution and reproduction in any medium, provided that the article is properly cited, the use is non-commercial and no modifications or adaptations are made.



**Amin Al Ka’bi** is an associate professor of electrical engineering at the Australian University in Kuwait. He was born in Jordan. He received his B.Sc. and M.Sc. degrees from the University of Jordan in 1989 and 1992 respectively, majoring in Electrical Engineering. He got his Ph.D. from the University of Queensland, Australia in 2006 in the field of electrical engineering/ communications. He has long industrial and academic experience in reputable industrial and academic institutions. His current research interests focus on wireless communication systems and signal processing.